

Seepage Analysis of Kiri Dam Using Finite Elements Method

Ahmed Bafeto Mohammed¹, Olugbenga Buari Elias Salau², Rose Daffi³, Amina Suleiman Gimba¹

¹Department of Civil Engineering Technology, The Federal Polytechnic, Damaturu, Nigeria

²Civil Engineering Department, Abubakar Tafawa Balewa University, Bauchi, Nigeria

³Civil Engineering Department, University of Jos, Nigeria

Corresponding author: Ahmed Bafeto Mohammed

-----ABSTRACT-----

Water impounded at the reservoir can be lost through many ways. The most important water lost through any embankment dam is seepage. Seepage depends on many factors including nature of construction materials, geometry of the dam body, reservoir water level, nature of the dam foundation and nature & efficiency of the seepage mitigation constructions like clay core and diaphragm wall. Seepage through Kiri is studied using finite element method by employing a software known as SEEP/W, 2007 developed by GeoSlope Studio. Four sections that include CH 685, CH 800, CH 1000 and CH 1100 are considered for analysis. On each section, 36 different reservoir elevations that include monthly reservoir elevations of 1984, 1997 and 2003 are considered. Seepage fluxes, hydraulic velocity and pore-water pressure are investigated. The results of the study revealed that both hydraulic velocity, seepage and pore-water pressures increase with the increase in reservoir elevation. From the analysis of the results the annual seepage computed for 1984, 1997 and 2003 are 17,152,165m³, 17,463,865m³ and 17,270,120m³ respectively which represents 2.779%, 2.840% and 2.808% loss of water in 1984, 1997 and 2003 from the reservoir that is meant to impound 615 million cubic meters. The velocity vectors are found to be concentrating much in the top layer of the foundation which has the peak hydraulic conductivity of 1.00E-6 m/s. They are also found to be mostly by-passing the clay core and the diaphragm wall for having least hydraulic conductivities. The pore-water pressure is negative, zero and positive at above the phreatic line, on the phreatic line and below the phreatic line respectively. In each case pore-water pressure peaked at the bottom of the foundation, upstream and least at the right end of the dam crest. Piping was observed not occurring. The dam is said to be safe for seeping less than 3% of its reservoir storage

Key words: Seepage, Piping, SEEP/W, Kiri Dam, hydraulic gradient, phreatic line, Pore-water Pressure

Date of Submission: 04-11-2019

Date Of Acceptance: 24-11-2019

I. INTRODUCTION

Dams are constructed across rivers or streams to impound water at the upstream to serve many purposes such as flood control, water supply, irrigation, fisheries, recreational activities and many more. Water impounded at the reservoir is lost through many ways. The most important ones include seepage, infiltration and evaporation (Fakhari and Ghanbari, 2013). Evaporation depends on the climatic conditions of the geographical location of the dam unlike infiltration that depends heavily on the geological condition of the reservoir foundation (Raghunath, 2006). On the other hand, seepage depends on many factors including nature of construction materials, geometry of the dam body, reservoir water level, nature of the dam foundation and nature and efficiency of the seepage mitigation constructions (Rushton and Redshaw 1979).

Seepage through an embankment dam is the movement of water through a porous medium from the upstream face of the dam to the downstream. Seepage always occurs in embankment dams. If the magnitude is beyond the design limits, it may harm the stability of the dam and drastically reduce the volume of the impounded water which may consequently cause the dam to fail meeting its targets. In embankment dam, stored water is lost through the dam body and through the foundation (Casagrande, 1937). All embankment dams have some seepage, because the impounded water, upstream, finds paths of least resistance through the dam and its foundation. Seepage becomes a concern if it is carrying embankment material with it, and should be controlled to prevent erosion of the embankment, or foundation, or damage to concrete structures (National Dam Safety Program Research Needs Workshop, 2006). Kiri dam, located in Guyuk L.G.A, Adamawa state, Nigeria is an embankment dam constructed in 1979. It is 1400m long, 20m high, zoned embankment with a central clay core and an upstream blanket. It is geographically located on 9°40'47"N 12°00'51"E (Udo, 1970). Kiri dam is constructed across Gongola River which is the principal tributary of the Benue River (Tukur and Mubi, 2002). Kiri dam is expected to impound about 615 million cubic meters of water.

Seepage has been implicated as the major cause of dam failure due to its potential to cause internal erosion of the embankment material (Lee, 2015). Different methods have been identified to study the extent of seepage in embankment dams. The problem of seepage in embankment dams contributes largely in a loss of stored water in the reservoir. This may lead to the defeat of the aim for which the dam was constructed if not properly taken care of.

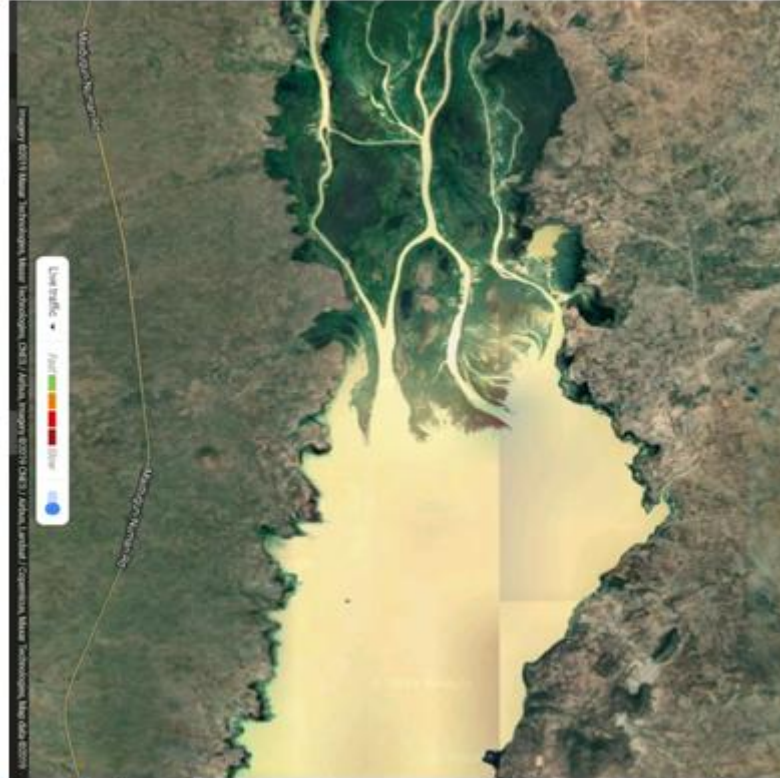


Figure 1: Kiri Dam Reservoir (Source: Google maps)



Figure 3: Upstream face of Kiri dam



Figure 2: Downstream face of the dam



Plate 4: Spillway gate of Kiri Dam

Kiri dam being an earth fill embankment dam may definitely face such a problem. Punmia and Lal, (1992), studied and made the following conclusions about the causes of dam failure. 40% of dam failure is attributed to hydraulic failures, 30% to seepage while structural failure carried the remaining 30%. Arora, (2001) also showed that about 35% of earth dam failures are due to hydraulic failures, stating that about 30% of

the failures are attributed to excessive seepage and about 20% are as a result of structural failures. The remaining 7% of the failures are due to other miscellaneous causes such as accidents and natural disasters. Seepage through an embankment dam may cause scouring and piping through the dam body, which, if not properly controlled, will cause dam settlement, thereby reducing the overall height of the dam body.

Depending on the type of the foundation, seepage through the foundation causes loss of stored water and piping which may cause settlement and subsequent dam failure. Different methods such as graphical and analytical methods have been employed in determining and analyzing seepage of various embankment dams in the world. The use of analytical methods involved lengthy numerical calculations that are time consuming and error oriented due to approximations in computations and plotting for graphical and analytical studies respectively. In this research work a computer method of study was employed. Different types of softwares are developed for analysing seepage. The one that has been employed in this research work was SEEP/W, 2007. It is selected to be used for its ability to handle both saturated and non-saturated conditions and for both steady and transient flow situation.

Seepage occurs through a permeable material which contains continuous voids (Craig, 2004). Materials such as rocks, soils etc. are permeable. The permeability of soils has a decisive effect on the stability of foundations, seepage loss through embankments of reservoirs, drainage of sub-grades, excavation of open cuts in water bearing sand and many others (Oosterbaan and Nijland, 1994).

Dam failures caused by seepage accounts for nearly 30% of all dam failures. The majority of such failures occur through the embankment or in the foundation (Darbandi et al, 2007). Seepage exists almost in all dams; however, showing different order of magnitudes and strengths. The seepage problem becomes so crucial if its rate increases abruptly and becomes uncontrollable (Darbandi et al, 2007).

Piping is one of the main causes of earth dam failures all over the world. It occurs due to the constant migration of soil particles towards free exits, or into coarse openings which might occur through the earth embankment or its foundation soil (Omofunmi et al, 2017). Piping accounts for approximately 50% of all earth dams' failures (Lee, 2015). The position of phreatic surface also determines the possibility of piping due to excessive gradient that is approaching unity. This causes softening and weakening of soil mass if it intersects the downstream slope (Dardabi et al, 2007). Another cause for piping is when the upstream material is of cohesive materials (materials of high permeability) (Dardabi et al, 2007).

SEEP/W is a finite element CAD software product for analyzing groundwater seepage and excess pore water pressure, dissipated problems with porous material such as soils and rocks.

SEEP/W can be used to model the movement and pore-water pressure distribution within porous material such as soil and rock. Its comprehensive formulation makes it possible to analyze both simple and complex seepage problems. SEEP/W has applications in the analysis and design of geotechnical, civil, hydrogeological, and mining engineering projects. It is also a general seepage analysis program that model both saturated and unsaturated flow. The ability to model unsaturated flows allows SEEP/W to handle a wider range of real problems than many other software products.

The inclusion of unsaturated flow in ground water modeling is important for obtaining physically realistic analysis result. In soils, the hydraulic conductivity and water stored changes as a function of pore-water pressure. SEEP/W models these relationships a continuous function. Most other seepage analysis software packages do not take these relationships in to account. They only use physically unrealistic assumptions that these functions are step functions. At a pore-water pressure of zero and above (ie below the water table), there's a saturated hydraulic conductivity value; at pore water pressures less than zero (above the water table), the hydraulic conductivity is zero. The use of such unrealistic functions to model soil hydraulic conductivity and water content can lead to error oriented results (SEEP/W, 2007).

SEEP/W is therefore recommended for use in the analysis of an embankment dam like the one in question i.e Kiri dam.

Different researchers such as Beheshti et al, 2013, Sazzad et al, 2015, Soleymani and Akhtarapur, 2011, Goharnejad et al, 2016, have used SEEP/W to analyse seepage of different dams. Their findings were presented in different approaches. (Beheshti et al, 2013) compared SEEP/W with a software called flac3d to analyse seepage through Gotvand-Olya Dam of various water levels from which results of almost similar magnitudes were obtained (Beheshti et al, 2013). It has been found using SEEP/W that mesh shape and size has negligible effect on the seepage. Seepage is independent of base permeability when core is not used. Type of base (pervious or impervious) affects the seepage for larger values of hydraulic conductivity when internal clay core is provided. When hydraulic conductivity is very small, base type has no effect on seepage (Sazzad et al, 2015). In Shurijeh dam, the total water quantity of flow obtained using SEEP/W, from dam body and foundation in the alluvial area with a cut-off wall was found to be 138m³/day (Soleymani and Akhtarapur, 2011). Same software revealed a seepage of 2.4498m³/s occurring through Dadin Kowa dam (Uloko, 2016).

Clay blanket has an effect on the seepage quantity of an embankment dam. Studies made on Farim-Sahra dam, Manzandran using SEEP/W without clay blanket revealed a seepage of 4.5937 x 10⁻⁴ (m³/s/m). With

lengths of clay blanket 150m (0.75m thick), 100m (0.33m thick) and 50m (0.10m thick) length, the seepage was computed by the software as $1.7011 \times 10^{-4}(\text{m}^3/\text{s}/\text{m})$, $3.2349 \times 10^{-4}(\text{m}^3/\text{s}/\text{m})$ and $3.6152 \times 10^{-4}(\text{m}^3/\text{s}/\text{m})$ respectively (Goharnejad et al, 2016).

Instrumentation and monitoring of dams and reservoirs are important concerns in dam engineering. At each stage of investigation, planning, design, construction, and operation in dam engineering, instrumentation and monitoring are required to monitor the behavior of engineering points. The performance of the dam during operations is aimed at safety of the dams and acquiring information to be used in progressing future design of dams. Instrumentation and monitoring are necessary in both the reservoir and the river basin, for normal operation and safety (Mizuno and Hirose, 2008). Kiri Dam is being monitored by various instrumentations that include hydraulic stand-pipes, pressure relief wells, drain holes in the inspection gallery, and stilling basins under drains. 9 stilling basins are installed at 0.6, 6.0, 11.0, 17.6, 23.0, 28.0, 34.6, 39.3 and 46.0m from the upstream end of the inspection gallery. Accurate calculations of seepage amount from body and foundation in dams are very important for economic and technical purposes. For the safety of dam, Seepage analysis in an embankment dam design is very important because the water flow in the body and foundation of a dam creates pore pressures and seepage forces (Soleymani and Akhtarpur, 2011).

II. MEHODOLOGY

2.1 Data Used

The data used for running the software are as follows:

2.2.1 Detailed drawings of the dam

These include:

- Section of the dam at 685m
- Section of the dam at 800m
- Section of the dam at 1000m and
- Section of the dam at 1100m

CH 685, CH 800 and CH 1000 are selected for the analysis for having most of the instrumentation facilities of the dam installed on them. Section at CH 1100 is selected for the analysis for having a unique berm length longer that is longer that all the rest.

2.1.2 Materials Properties of the Dam and its Foundation

The foundation of Kiri dam consists of thick alluvium deposit of about 65m depth under lain by bed rock with Bima sandstone as its main geological formation. The oldest material is consolidated, gray to dark gray, dense silty and silty clay, topped by a cemented nebula and grit conglomerate at a depth below river bed of 31 to 35 meters. The younger layer of alluvium occupies a belt of about 375 meters wide and about 16 meters thick, comprising of sand and clays, mostly silty. Above this again, is a third layer of sandy silts and clays of about 15 meters thin of loose, mainly occupying a broad belt of 700 meters wide. Finally, there's a top layer of 3m sandy alluvium, eroded away completely except on the present banks and lying everywhere above the present river bed level.

Table 1: Geological formation of Kiri Dam foundation

Formation Type	Depth from the Bed Rock(m)	Thickness	Hydraulic Conductivity (m/s)
Older layer of dark gray, dense silty sand and silty clay	0 – 32	35	1.5E-08
Younger Layer of silty sand and silty clay	32 – 48	16	2.65E-07
Sandy silts and clays	48 – 63	15	1.40E-7
Compacted sand	63 – 65	3	1.00E-6

Source: (WardAshcroft and Parkman Nig. 1977).

2.1.3 Materials Properties of the Embankment Materials (Hydraulic Conductivity)

Hydraulic conductivities of the construction materials are factors that are mainly responsible for the magnitudes of seepage velocity through embankment materials. The lower the conductivity values of the materials the lesser ability of the embankment material to allow the passage of seeping water and vise-versa. Therefore, embankment materials with low conductivities (clays and silty clays) are used as core and/or upstream clay blanket to minimize seepage. The embankment materials used in the construction of the dam have the following hydraulic conductivities

Table 2: Hydraulic conductivities of the construction materials

S/N	Material Type	Hydraulic conductivity(m/s)
1	Central clay core (Impervious Clay Core)	8.04E-09
2	Upstream blanket (Impervious Clayey Sand)	5.00E-07
3	Embankment (Pervious sand shell)	1.00E-06
4	Diaphragm wall (Impervious Clay)	7.00E-10

Source: (WardAshcroft and Parkman Nig. 1977)

Analysis Procedure

2.1.4 Problem definition

The procedure followed for achieving the seepage analysis using SEEP/W was as follows:

Setting the Working Space: The working area used for this analysis was 840mm width and 594mm high. A scale of 1:500 was used in both vertical and horizontal axes. Linear dimensions are set in meters while unit weight of water was considered as 9.80 kN/m³. A grid spacing of 1m was adopted in order to conveniently sketch the dam geometries.

Sketching the Problem: In defining a finite element problem, the problem dimensions were first of all prepared. The ‘sketch menu’ was used as a guide for drawing the problem regions and defining its boundary conditions.

Generating Regions: In this analysis, 8 regions were generated

- Clay core
- Upstream blanket
- Diaphragm wall
- Pervious sand shell
- Foundation 1 (Older layer of dark gray, dense silty sand and silty clay)
- Foundation 2 (Younger Layer of silty sand and silty clay)
- Foundation 3 (Sandy silts and clays)
- Foundation 4 (Compacted sand)

Defining Materials’ Properties (Hydraulic Conductivity). Just as shown above, analyzing seepage through Kiri Dam involved the consideration of 8 regions. Each region has a hydraulic conductivity value that was defined. SEEP/W (2007) considered all the regions depending on its position and thickness to predict a seepage value through the dam in form of a volumetric rate. Hydraulic conductivity of the materials are as stated on table 3

Table 3: Material properties of the dam and its foundation

S/N	Material Type	Hydraulic conductivity(m/s)
1	Clay Core	8.04E-09
2	Upstream blanket	5.00E-07
3	Embankment	1.00E-06
4	Diaphragm wall	7.00E-10
5	Foundation 1	1.5E -08
6	Foundation2	2.65E-07
7	Foundation 3	1.40E-7
8	Foundation 4	1.00E-6

Drawing regions: On each section, eight regions are drawn. They include four foundation regions, diaphragm wall, central clay core, upstream blanket and main embankment material region.

Defining Boundary Conditions: The following boundary conditions were considered for the analysis

- Reservoir elevations of the 36 months (January to December in 1984, 1997 and 2003) measured by the dam operators were used for the analysis of sections at chainages 685m, 800m, 1000m and 1100m. the elevations ranges between 167.02m to 170.97m above mean sea level with free boards ranging between 3.53m and 7.48m
- Zero pressure boundary is considered at the downstream toe
- Potential seepage surface boundary condition is applied to the downstream face of the dam. This is called a potential seepage face. It is a special boundary condition that is used to locate where the seepage face might develop.

Creating Finite Element Mesh: A triangular pattern of meshing was adopted with each side of the triangle considered to be 3m. This was applied for 8 regions. The triangular pattern is selected to ease the meshing of the triangular oriented regions of the dam. Rectangular quads will be suitable.

Verifying and Solving the Problem: The software (SEEP/W) allowed for verifying all the keyed-in data to ensure correctness of the entry and modifications where necessary. In the dialog list box, messages appear stating the verification steps performed. Necessary corrections were made.

Viewing the Results: Before printing the results, SEEP/W allowed viewing the results in a graphical form by:

- Generating all contour plots
- Displaying the velocity vectors which represents the flow directions and maximum hydraulic velocities.
- Displaying the flow paths. These path does not mean flow lines like those of flow net, instead, they indicate a predicted path through which a drop of water will flow from the reservoir to the downstream side of the dam and/or its foundation.
- Displaying the seepage flux
- Displaying the pore-water pressure results at any point selected

Figures 5, 6, 7 and 8 show a problem definition of the dam section at Chainage 685, 800, 1000 and 1100m respectively.

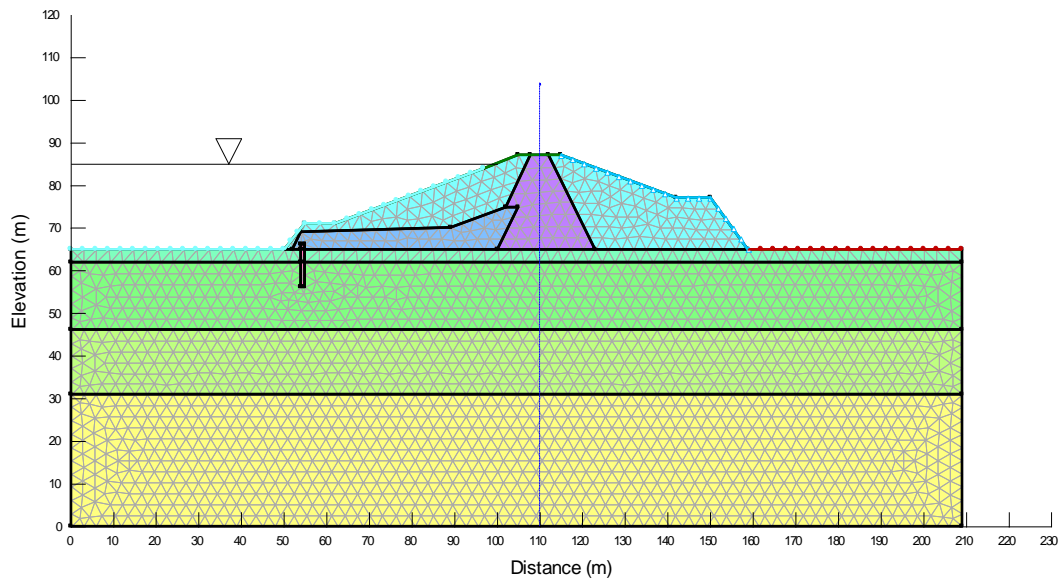


Figure 5: Problem definition of Kiri dam section at chainage 685m

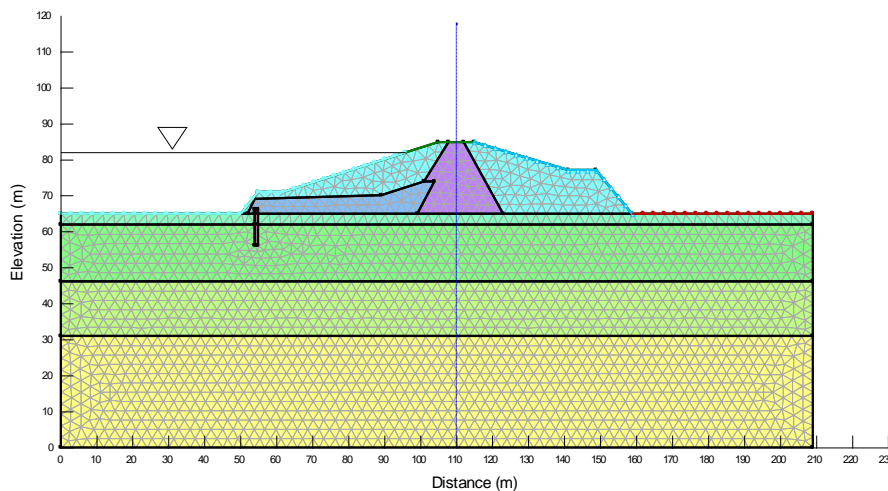


Figure 6: Problem definition of Kiri dam section at chainage 800m

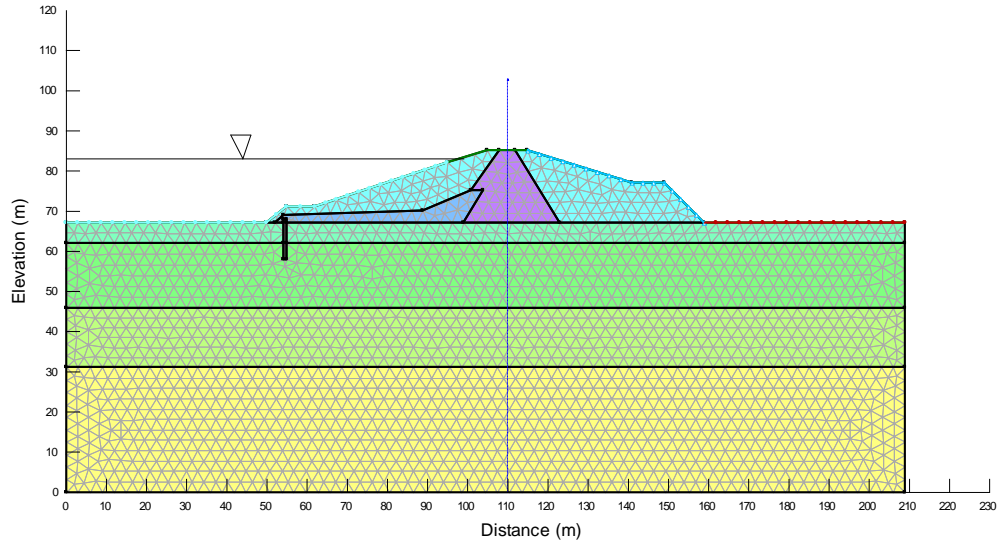


Figure 7: Problem definition of Kiri dam section at chainage 1000m

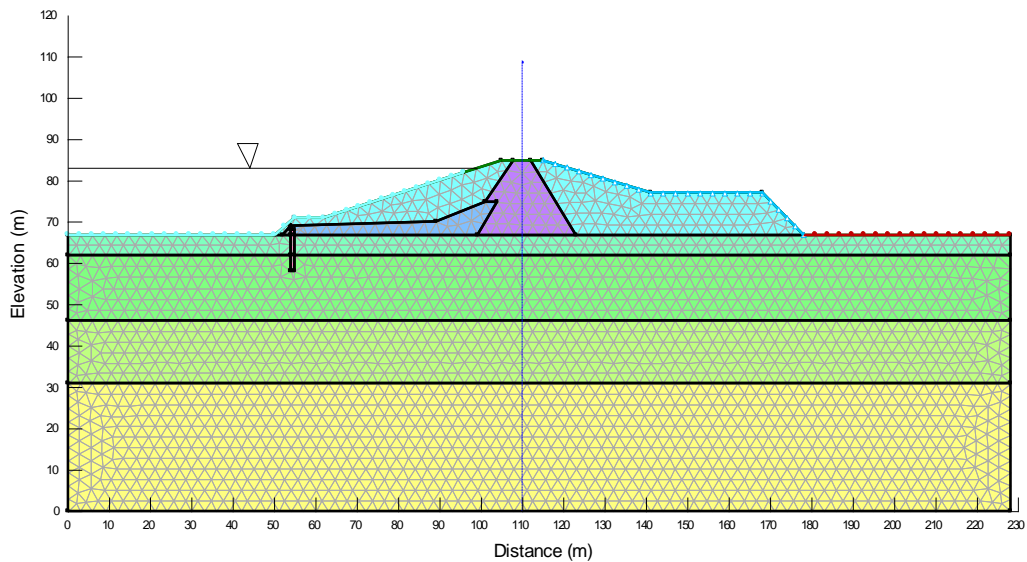


Figure 8: Problem definition of Kiri dam section at chainage 1100m

III. RESULTS AND DISCSSIONS

3.1 Velocity Fields

The maximum velocity of flow through the dam was tested for the six sections in question and for all the 12 months of the 3 studied years. The results are tabulated in table 4.

The velocity vectors of the seeping water for the month of May with a reservoir elevation 170.97m are graphically displayed on figure 17, figure 18, figure 19, figure 20, figure 21, figure 22, for CH600, CH685, CH800, CH880, CH1000 and CH 1100 respectively. Month of May, 1997 is selected for the display for having the maximum reservoir elevation in all the cases.

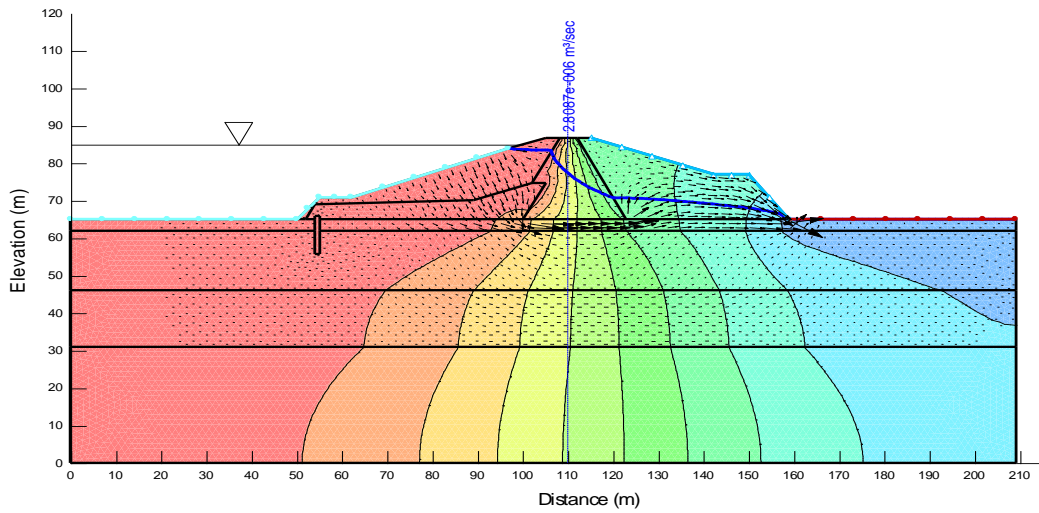


Figure 9: Flow path/velocity vectors of seepage at Ch685

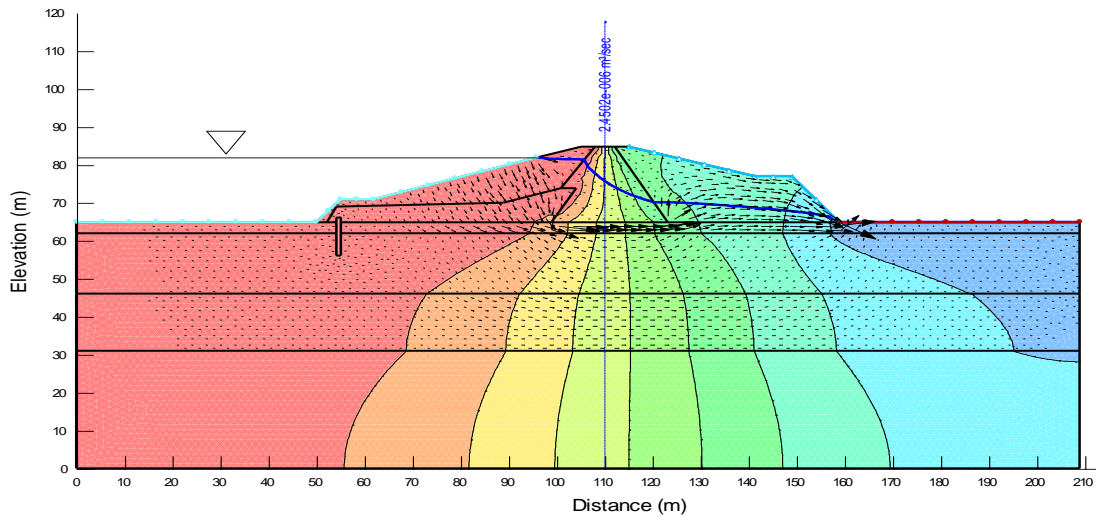


Figure 10: Flow path/velocity vectors of seepage at Ch800

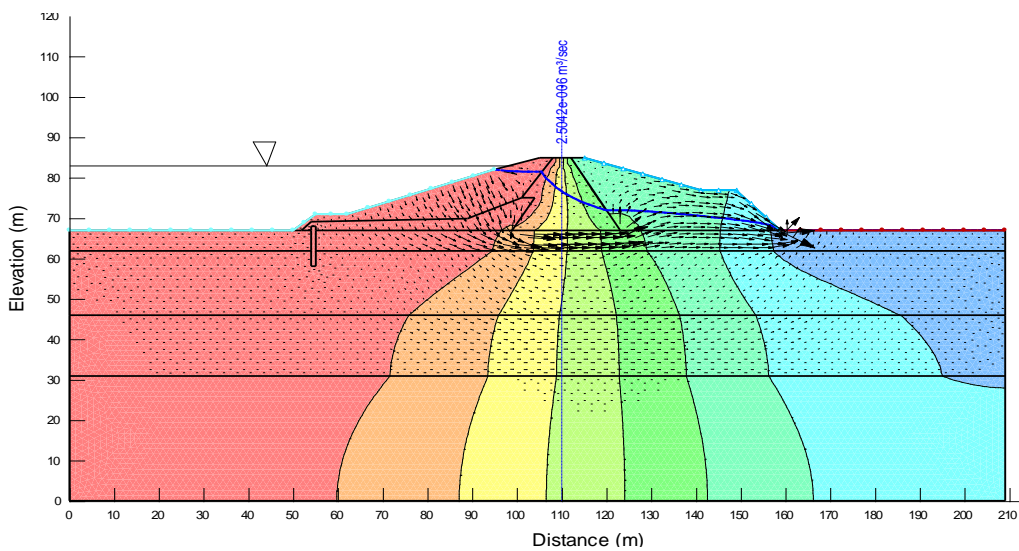


Figure 11: Flow path/velocity vectors of seepage at Ch1000

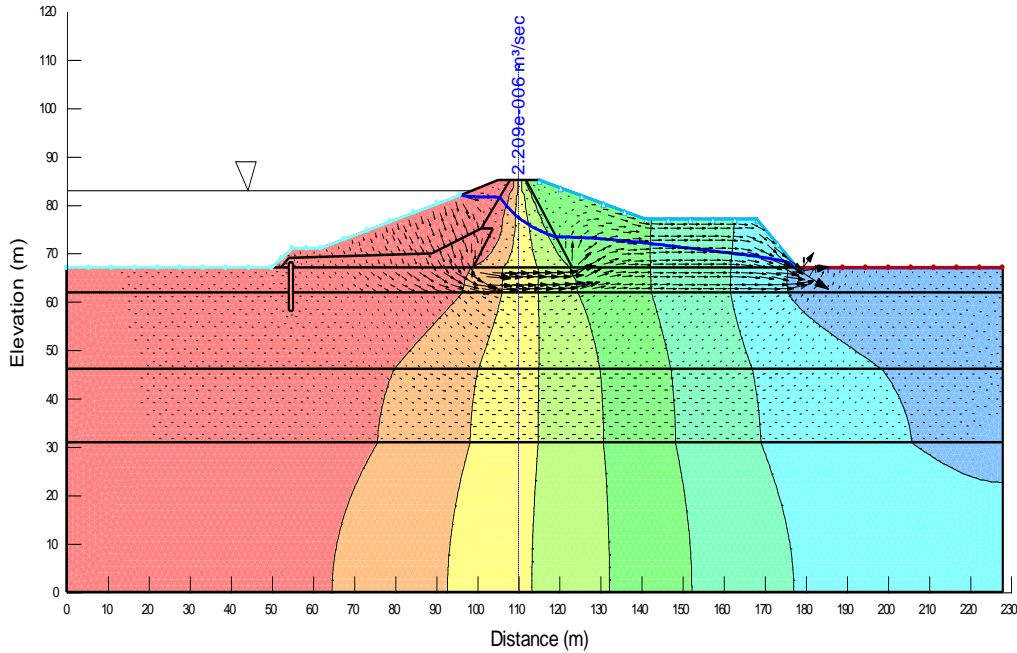


Figure 12: Flow path/velocity vectors of seepage at Ch1100

Table 4: Comparison between hydraulic velocities for different sections

Year	Month	Maximum Pore-water pressure (kPa)				
		Reservoir Elevation (m)	CHAINAGE (m)			
			CH 685	CH 800	CH 1000	CH 1100
1984	January	170.37	5.5935E-07	4.8421E-07	4.4951E-07	4.00474E-07
	February	170.34	5.5770E-07	4.8410E-07	4.4716E-07	3.99667E-07
	March	170.16	5.5191E-07	4.7866E-07	4.4169E-07	3.94761E-07
	April	169.85	5.4225E-07	4.6876E-07	4.3084E-07	3.85181E-07
	May	169.74	5.3899E-07	4.6525E-07	4.2761E-07	3.83703E-07
	June	167.02	4.5055E-07	3.7615E-07	3.2938E-07	2.95675E-07
	July	169.32	5.2347E-07	4.4993E-07	4.1497E-07	3.69007E-07
	August	168.55	5.0059E-07	4.2655E-07	3.8440E-07	3.44207E-07
	September	167.82	4.7684E-07	4.0290E-07	3.5848E-07	3.21335E-07
	October	170.31	5.5723E-07	4.8328E-07	4.4624E-07	3.98849E-07
	November	170.57	5.6775E-07	4.9149E-07	4.5560E-07	4.07088E-07
	December	170.31	5.5723E-07	4.8328E-07	4.4624E-07	3.98849E-07
1997	January	170.54	5.6597E-07	4.9071E-07	4.5468E-07	4.06271E-07
	February	170.39	5.5947E-07	4.8581E-07	4.4867E-07	4.03231E-07
	March	170.34	5.5797E-07	4.8429E-07	4.4716E-07	3.97717E-07
	April	170.17	5.5258E-07	4.7892E-07	4.4199E-07	3.95034E-07
	May	170.97	5.7783E-07	5.0405E-07	4.6931E-07	4.1909E-07
	June	168.55	5.0059E-07	4.2655E-07	3.8440E-07	3.44207E-07
	July	168.55	5.0059E-07	4.2724E-07	3.8440E-07	3.44207E-07
	August	168.24	4.8725E-07	4.1334E-07	3.7006E-07	3.31534E-07
	September	168.65	5.0400E-07	4.2992E-07	3.8743E-07	3.46932E-07
	October	170.28	5.5594E-07	4.8242E-07	4.4533E-07	3.98032E-07
	November	170.11	5.5028E-07	4.7709E-07	4.3913E-07	3.92571E-07
	December	170.29	5.5627E-07	4.8270E-07	4.4129E-07	3.98304E-07
2003	January	170.23	5.5450E-07	4.8069E-07	4.4382E-07	3.96669E-07
	February	170.01	5.4754E-07	4.7374E-07	4.3609E-07	3.89845E-07
	March	169.98	5.4654E-07	4.7298E-07	4.3518E-07	3.89845E-07
	April	169.84	5.4529E-07	4.6853E-07	4.3053E-07	3.84908E-07
	May	169.58	5.3737E-07	4.6022E-07	4.2085E-07	3.76397E-07
	June	168.89	5.1262E-07	4.3781E-07	3.9668E-07	3.55035E-07
	July	168.56	5.0195E-07	4.2682E-07	3.8468E-07	3.44469E-07
	August	168.19	4.8828E-07	4.1491E-07	3.7158E-07	3.32897E-07
	September	170.2	5.5156E-07	4.8300E-07	4.4594E-07	3.9973E-07
	October	170.26	5.5740E-07	4.8093E-07	4.4555E-07	4.00631E-07
	November	169.7	5.3845E-07	4.6196E-07	4.3232E-07	3.86502E-07
	December	169.96	5.4982E-07	4.7233E-07	4.3416E-07	3.88158E-07

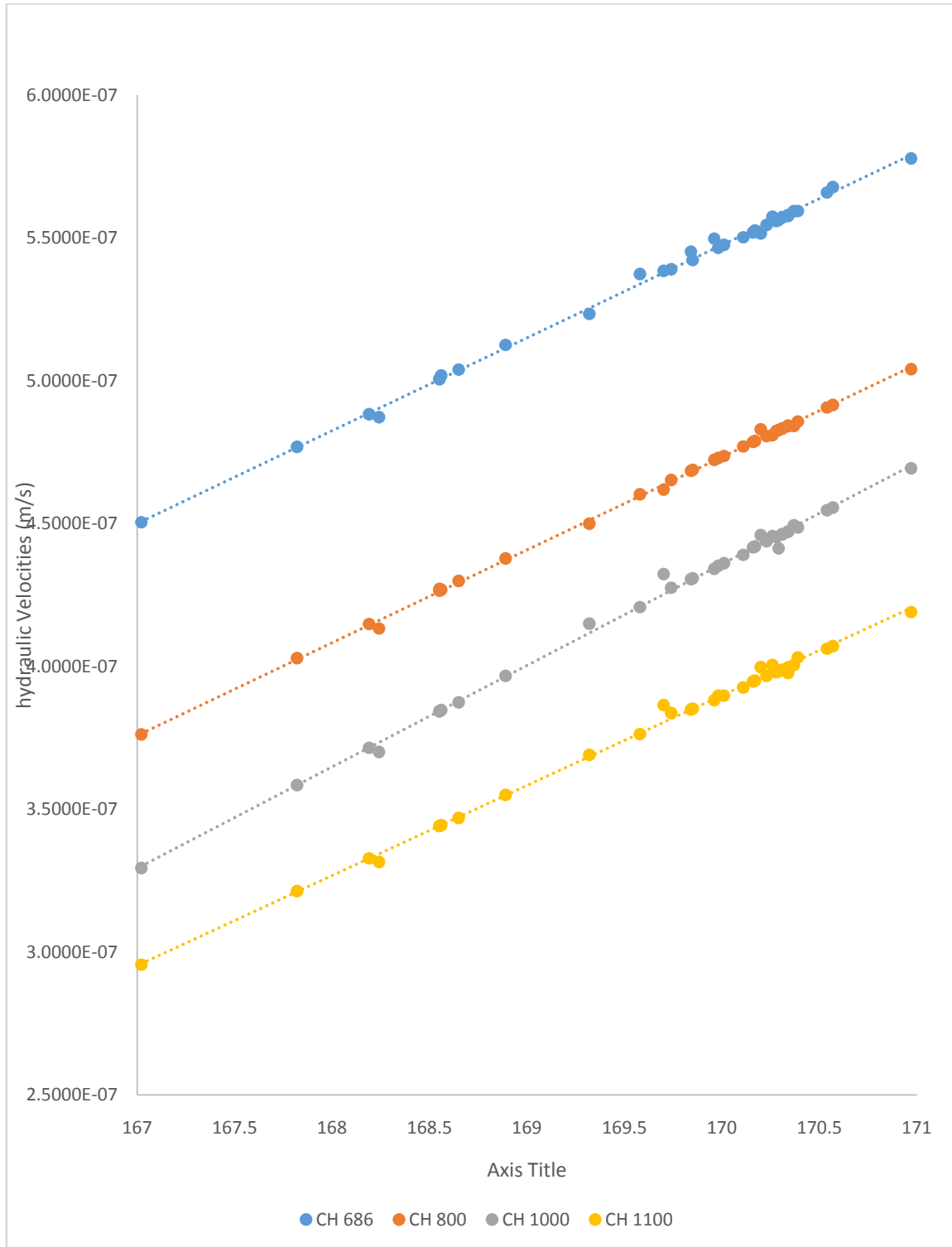


Figure 13: Hydraulic velocity in relation to reservoir elevation for CH 685

The hydraulic velocities are plotted against the reservoir elevations. As can be seen on figure 13, the magnitudes of the velocities increase with the increase in reservoir elevation. This shows that more portion of the embankment material is wet as the reservoir elevation increases thereby increasing the seepage velocity. The seeping rate of the impounded water is directly proportional to its hydraulic velocity in each case.

SEEP/W compiled the hydraulic conductivities of all the regions in accordance to the magnitude of the conductivities and the total area of each region to compute the general maximum hydraulic velocity of the entire section.

It can be observed from the velocity vectors that the seeping water find their ways away from the diaphragm wall and the central clay core for having very low hydraulic conductivities. This indicted that the essence of providing a soil material with low permeability to mitigate seepage has provided a reasonable effect.

The flow particles are mostly seeping through the embankment and a foundation layer with low permeability. Negligible amount of seeping particles seeps above the phreatic surface where the negative pore-water pressure exists. Above the phreatic line it is always expected to be dry if not because of capillarity action. The velocity vectors concentrated much at the embankment material and at the foundation that has a higher conductivity by-passing those regions with lower conductivities.

Velocity vectors seem to appear at toe of the dam. The seeping water is collected at the toe drain and to some extent in the pressure relief wells.

3.2 Seepage

Table 5: Comparison between Seepage fluxes for different sections

Year	Month	Seepage Flux ($m^3/s/m^2$)				
		Reservoir Elevation (m)	CH 685	CH 800	CH 1000	CH 1100
1984	January	170.37	2.7063E-06	2.3320E-06	2.3791E-06	2.0946E-06
	February	170.34	2.6887E-06	2.3303E-06	2.3550E-06	2.0806E-06
	March	170.16	2.6544E-06	2.3015E-06	2.3244E-06	2.0535E-06
	April	169.85	2.6009E-06	2.2436E-06	2.2620E-06	1.9927E-06
	May	169.74	2.5844E-06	2.2234E-06	2.2376E-06	1.9619E-06
	June	167.02	2.0939E-06	1.7651E-06	1.6608E-06	1.4733E-06
	July	169.32	2.4795E-06	2.1264E-06	2.1267E-06	1.8650E-06
	August	168.55	2.3660E-06	2.0055E-06	1.9720E-06	1.7453E-06
	September	167.82	2.2353E-06	1.8779E-06	1.8243E-06	1.6148E-06
	October	170.31	2.7015E-06	2.3276E-06	2.3498E-06	2.0760E-06
	November	170.57	2.7210E-06	2.3754E-06	2.4135E-06	2.1318E-06
	December	170.31	2.7015E-06	2.3276E-06	2.3498E-06	2.0760E-06
1997	January	170.54	2.7210E-06	2.3726E-06	2.4084E-06	2.1272E-06
	February	170.39	2.7008E-06	2.3414E-06	2.3635E-06	2.1043E-06
	March	170.34	2.6929E-06	2.3332E-06	2.3550E-06	2.0924E-06
	April	170.17	2.6617E-06	2.3025E-06	2.3261E-06	2.0550E-06
	May	170.97	2.8087E-06	2.4502E-06	2.5042E-06	2.2090E-06
	June	168.55	2.3660E-06	2.0055E-06	1.9720E-06	1.7453E-06
	July	168.55	2.3660E-06	1.9930E-06	1.9720E-06	1.7453E-06
	August	168.24	2.3110E-06	1.9337E-06	1.8894E-06	1.6730E-06
	September	168.65	2.3860E-06	2.0240E-06	1.9887E-06	1.7601E-06
	October	170.28	2.6800E-06	2.3224E-06	2.3447E-06	2.0715E-06
	November	170.11	2.6456E-06	2.2923E-06	2.3035E-06	2.0355E-06
	December	170.29	2.7063E-06	2.3115E-06	2.3340E-06	2.0730E-06
2003	January	170.23	2.6733E-06	2.3239E-06	2.3365E-06	2.0642E-06
	February	170.01	2.6332E-06	2.2713E-06	2.2863E-06	2.0203E-06
	March	169.98	2.6269E-06	2.2688E-06	2.2814E-06	2.0118E-06
	April	169.84	2.6008E-06	2.2430E-06	2.2532E-06	1.9912E-06
	May	169.58	2.5531E-06	2.1948E-06	2.1907E-06	1.9367E-06
	June	168.89	2.4009E-06	2.0678E-06	2.0447E-06	1.8088E-06
	July	168.56	2.3682E-06	2.0066E-06	1.9735E-06	1.7466E-06
	August	168.19	2.2994E-06	1.9419E-06	1.8978E-06	1.6804E-06
	September	170.2	2.6866E-06	2.3254E-06	2.3482E-06	2.0526E-06
	October	170.26	2.6689E-06	2.3155E-06	2.3076E-06	2.0499E-06
	November	169.7	2.5837E-06	2.2106E-06	2.2626E-06	1.9519E-06
	December	169.96	2.6215E-06	2.2648E-06	2.2732E-06	2.0089E-06

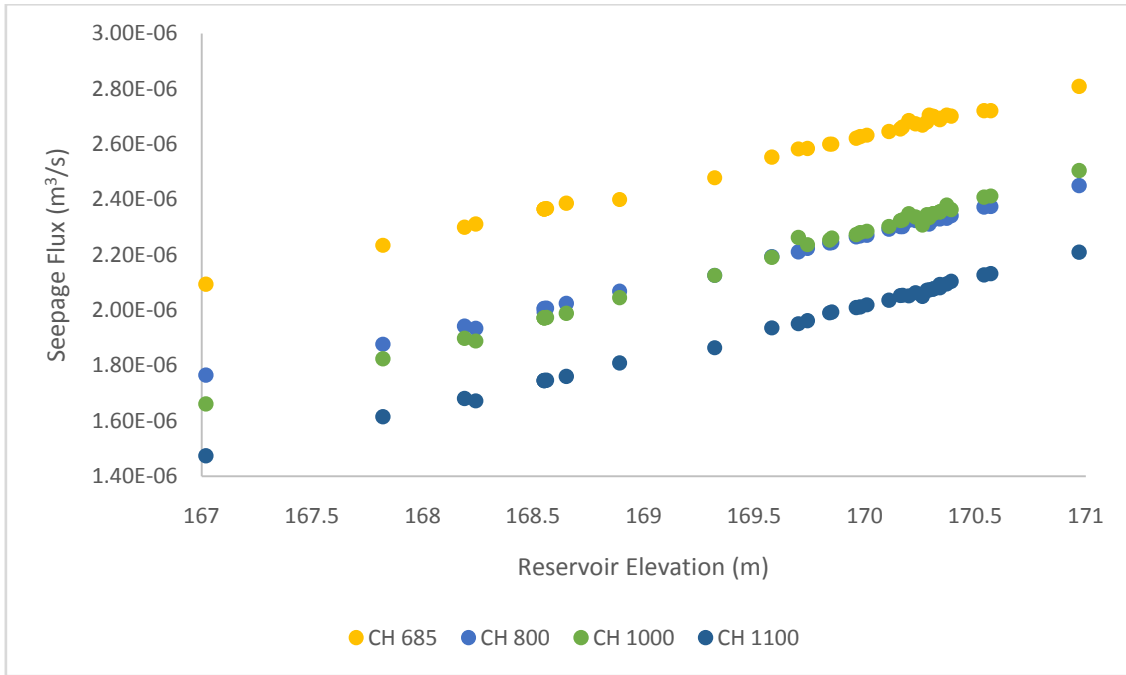


Figure 14: Seepage in relation to reservoir elevation for CH 1100

Table 6: Cross-sectional areas of the studied sections

Section	Number of nodes	Number of Elements	Area of Section (m ²)
685	2058	3927	19757
800	2040	3892	19581
1000	2082	3975	19999
1100	2264	4327	21770

Table 7: Average monthly seepage

Year	Month	Res. Elevation (m)	Average seepage (m ³ /s/m ²)	Average seepage (m ³ /s)	Annual seepage (m ³ /s)	Annual Seepage (m ³ /year)	Percentage water loss due to seepage
1984	January	170.37	2.43E-06	4.86E-02	5.44E-01	17,152,165	2.779
	February	170.34	2.41E-06	4.83E-02			
	March	170.16	2.38E-06	4.77E-02			
	April	169.85	2.32E-06	4.65E-02			
	May	169.74	2.30E-06	4.61E-02			
	June	167.02	1.81E-06	3.62E-02			
	July	169.32	2.20E-06	4.41E-02			
	August	168.55	2.08E-06	4.16E-02			
	September	167.82	1.94E-06	3.89E-02			
	October	170.31	2.41E-06	4.83E-02			
	November	170.57	2.46E-06	4.92E-02			
	December	170.31	2.41E-06	4.83E-02			
1997	January	170.54	2.45E-06	4.92E-02	5.54E-01	17,463,865	2.840
	February	170.39	2.43E-06	4.86E-02			
	March	170.34	2.42E-06	4.84E-02			
	April	170.17	2.38E-06	4.78E-02			

	May	170.97	2.54E-06	5.09E-02			
	June	168.55	2.08E-06	4.16E-02			
	July	168.55	2.07E-06	4.15E-02			
	August	168.24	2.01E-06	4.02E-02			
	September	168.65	2.09E-06	4.19E-02			
	October	170.28	2.40E-06	4.81E-02			
	November	170.11	2.37E-06	4.74E-02			
	December	170.29	2.41E-06	4.82E-02			
2003	January	170.23	2.40E-06	4.81E-02	5.48E-01	17,270,120	2.808
	February	170.01	2.35E-06	4.71E-02			
	March	169.98	2.35E-06	4.70E-02			
	April	169.84	2.32E-06	4.65E-02			
	May	169.58	2.27E-06	4.55E-02			
	June	168.89	2.13E-06	4.27E-02			
	July	168.56	2.08E-06	4.16E-02			
	August	168.19	2.01E-06	4.02E-02			
	September	170.2	2.40E-06	4.81E-02			
	October	170.26	2.39E-06	4.78E-02			
	November	169.7	2.30E-06	4.61E-02			
	December	169.96	2.34E-06	4.69E-02			

Table 7 Shows results of seepage flux through the four analysed sections using the reservoir elevations for all the 12 months of 1984, 1997 and 2003. The seepage results are compared to the reservoir elevation for all the four sections. The trend is uniformly linear. Consequently, in all the cases, seepage flux increases with the increase in reservoir elevation.

Relatively, higher seepage flux values are recorded at CH 685, followed by CH 800 then CH 1000 and least at CH 1100 with their peaks at May, 1997 for having a reservoir elevation of 170.97m.

In 1984, the seepage magnitudes obtained were summed to a tune of $5.440E-01m^3/s$ which is $60 \times 60 \times 24 \times 365 \times 5.44E-01 m^3/year$, amounting to $17,152,165m^3/year$. This represents 2.779% of the annual storage of the reservoir that is meant to impound 615 million cubic meters

In 1997, the seepage magnitudes obtained were summed to a tune of $5.54E-01m^3/s$ which is $60 \times 60 \times 24 \times 365 \times 5.54E-01 m^3/year$, amounting to $17,463,865 m^3/year$. This represents 2.840% of the annual storage of the reservoir that is meant to impound 615 million cubic meters

In 2003, the seepage magnitudes obtained were summed to a tune of $5.48E-01m^3/s$ which is $60 \times 60 \times 24 \times 365 \times 5.48E-01 m^3/year$, amounting to $17,270,120m^3/year$. This represents 2.808% of the annual storage of the reservoir that is meant to impound 615 million cubic meters.

In a dam with crest width 8m, height of 15m and a reservoir depth of 13m and a hydraulic conductivity $1.00E-6m/s$, Casagrande, Scharffenak (1917) and Stello's formulae (1987) found seepage to be $2.9391E-6$, $5.00E-6$, $4.16E-6m^3/s$ respectively. Same parameters were used by Fakhari and Gambari (2013) in SEEP/W and computed seepage to be $4.4331E-6m^3/s$. using Resk and Noon (2011) formulae, the seepage through the dam is $1.0715E-7m^3/s$.

Kiri dam has 13 drain holes in the spillway gallery, 9 stilling basin under-drains in the low head gallery, stationed at different chainages and elevation to monitor seepage. The total seepage observed in June, 2003 was $2.30E-05m^3/s$. Using June, 2003 reservoir elevation of 168.89m seepage flux were computed using SEEP/W to be $2.4009E-06m^3/s$, $2.0678E-06m^3/s$, $2.0447E-06m^3/s$ and $1.8088E-06m^3/s$ on Ch685, Ch800, Ch1000 and Ch1100 respectively, which is $2.13 E-06m^3/s$ on average. The SEEP/W computation is about 10 times less than that of the manually measured seepage.

4.4 Pore-water pressure distribution results

The pore-water pressure distribution of the four sections are displayed on figure 15, Figure 16, Figure 17 and Figure 18.

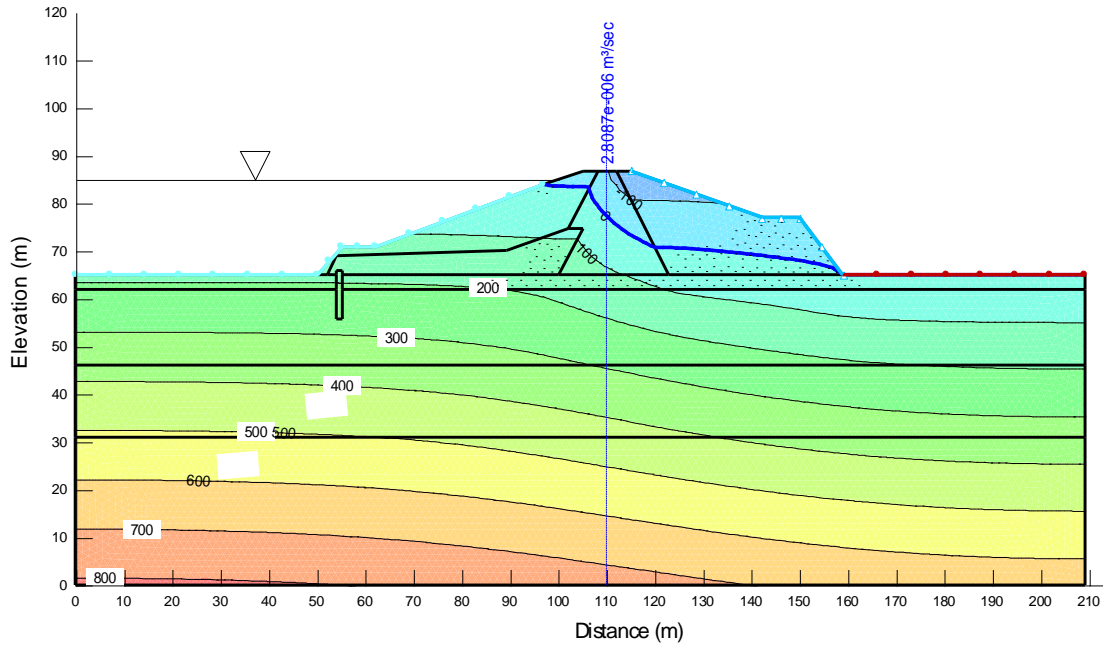


Figure 15: pore-water pressure distribution for CH 685

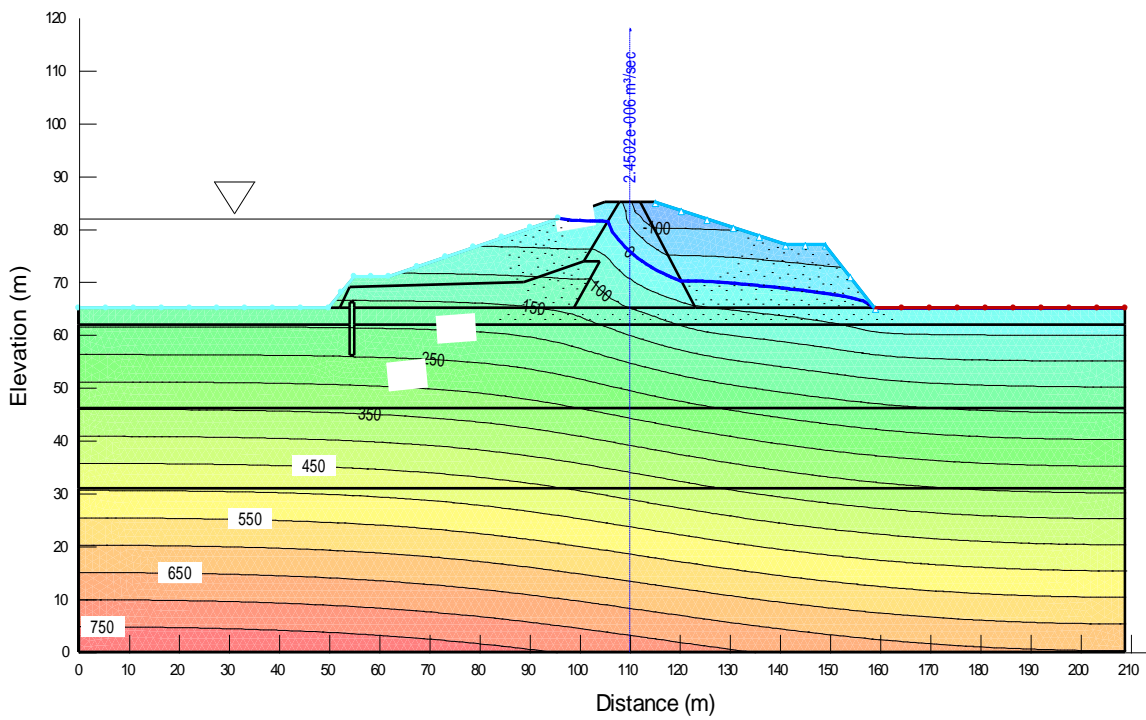


Figure 16: pore-water pressure distribution for CH 800

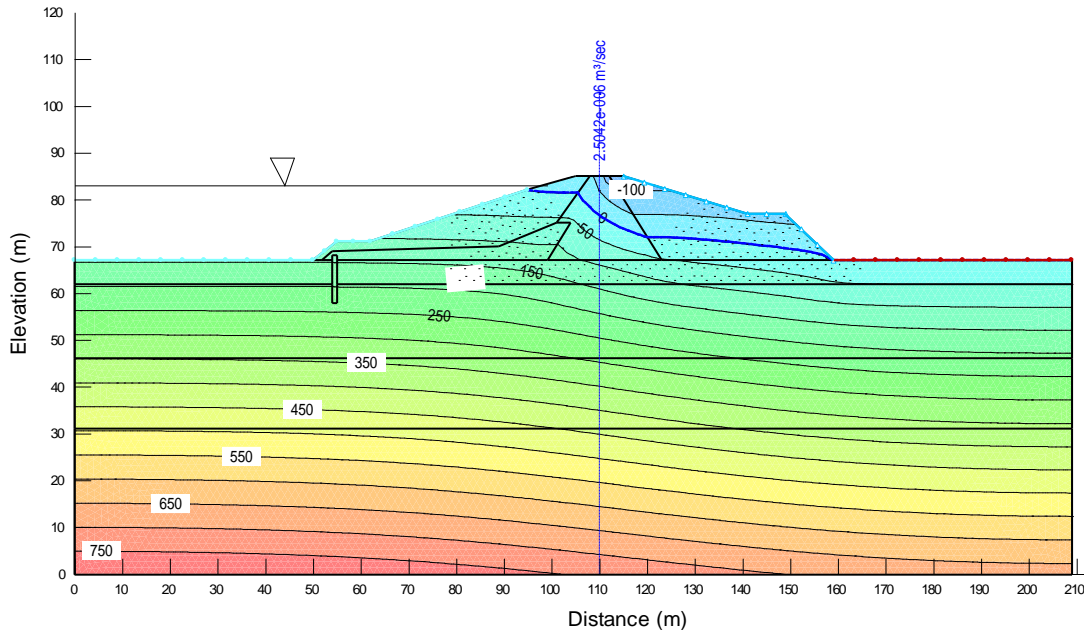


Figure17: pore-water pressure distribution for CH 1000

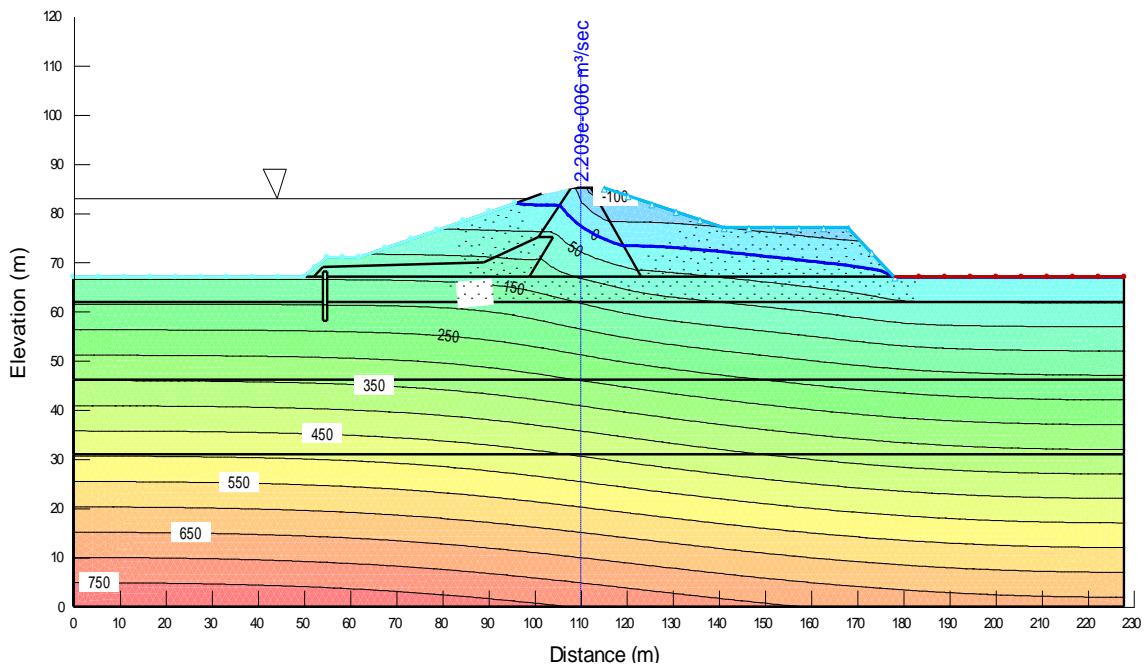


Figure 18: pore-water pressure distribution for CH 1100

Table 8: Comparison between maximum pore-water pressures for different sections

Year	Month	Maximum Pore-water pressure (kPa)				
		Reservoir Elevation (m)	CHAINAGE (m)			
			CH 685	CH 800	CH 1000	CH 1100
1984	January	170.37	811	792	790	790
	February	170.34	811	792	789	790
	March	170.16	809	790	788	788
	April	169.85	806	788	785	786
	May	169.74	805	786	784	784
	June	167.02	779	760	758	759
	July	169.32	801	783	780	781
	August	168.55	794	775	773	773
	September	167.82	787	768	765	766
	October	170.31	811	792	789	790
	November	170.57	813	794	792	792
	December	170.31	811	792	789	790
1997	January	170.54	812	794	791	792
	February	170.39	812	793	790	791
	March	170.34	811	792	789	790
	April	170.17	809	790	788	789
	May	170.97	817	798	795	796
	June	168.55	794	775	773	773
	July	168.55	794	775	773	773
	August	168.24	791	772	769	770
	September	168.65	795	776	774	774
	October	170.28	811	791	789	790
	November	170.11	808	790	787	788
	December	170.29	810	791	789	790
2003	January	170.23	810	792	788	789
	February	170.01	808	789	786	787
	March	169.98	808	789	786	787
	April	169.84	806	787	785	785
	May	169.58	804	785	782	783
	June	168.89	797	778	776	777
	July	168.56	794	775	773	773
	August	168.19	791	772	769	770
	September	170.2	810	792	789	790
	October	170.26	810	792	787	789
	November	169.7	805	786	783	784
	December	169.96	807	788	786	787

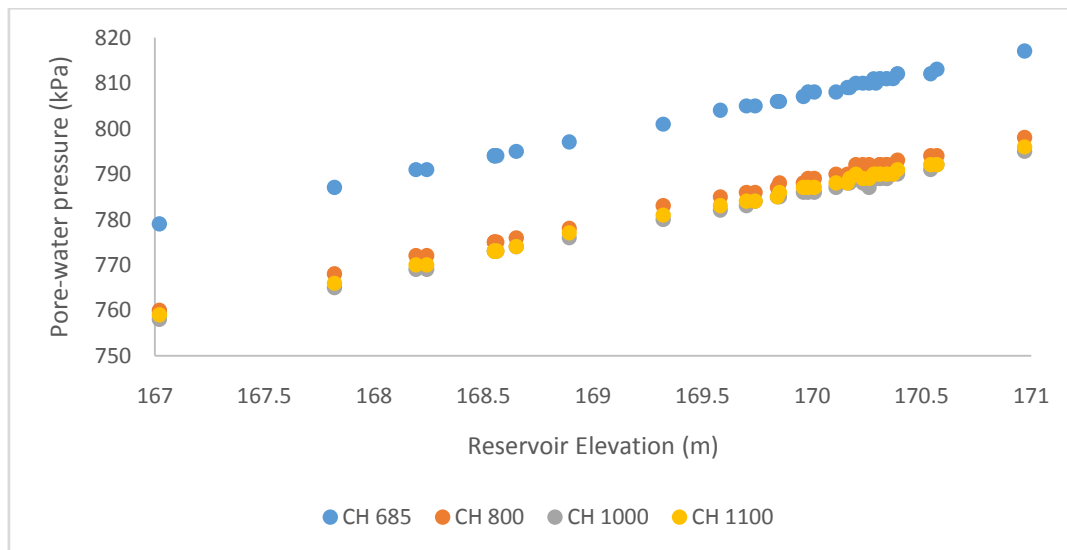


Figure 19: Pore-water pressure in relation to Reservoir Elevation for CH 685

The pore-water pressure distribution across the dam and its foundation has common pattern for all the analysed sections. The most notable patterns are that:

- Minimum pore-water pressure exist at the right corner of the dam crest
- Maximum pore-water pressure exist at the left bottom end of the foundations
- Zero pore-water pressure occur on the phreatic line, above which, the pressure is negative and below which, the pressure is positive.

29 hydraulic piezometers are installed on the dam, 9 on CH 685, 11 on CH 800 and 9 on Ch 1000. They are installed at different chainages and elevations as can be seen on table 9, table 10 and table 11. Corresponding pore-water pressures are computed using SEEP/W using May 1997 reservoir elevation of 170.97m. The results are compared to the measured pore-water pressure as at July, 2007 with a reservoir elevation of May 1997 and the results are also tabulated on the same table.

Table 9: Comparison between the direct measurement of pressure head and SEEP/W for CH 685

Piezometer number	Offset from the center line (m)	Elevation (m)	Coordinates on the SEEP/W solution	Manually Measured Pressure Head (m)	SEEP/W Computed Pressure Head (m)
H1	3.4U/S	165.96	107.66,77.96	-39.04	-41.08
H2	0.0	165.87	110.00,77.87	-30.41	-31.56
H3	5.0 U/S	158.00	105.00,70.00	35.61	37.83
H4	0.00 U/S	158.00	110.00,70.00	38.55	39.34
H5	6.0 U/S	158.00	117.00,70.00	29.23	30.52
H6	47.5 U/S	151.99	62.50,63.99	88.19	89.74
H7	24.0 U/S	152.08	86.00,64.08	79.95	82.92
H8	4.0 U/S	152.21	106.00,64.21	68.87	68.33
H9	47.5 U/S	144.00	62.50,56.00	164.61	165.14

Table 10: Comparison between the direct measurement of pressure head and SEEP/W for CH 800

Piezometer number	Offset from the center line (m)	Elevation (m)	Coordinates on the SEEP/W solution	Manually Measured Pressure Head (m)	SEEP/W Computed Pressure Head (m)
H10	2.00 U/S	166.98	108.00,77.96	-56.51	-53.15
H11	0.00	167.03	110.00,79.03	-57.00	-50.99
H12	4.67 U/S	158.99	105.33,70.99	21.88	24.84
H13	0.00	158.99	110.00,70.99	21.88	23.00
H14	5.00 D/S	158.99	117.00,70.99	21.88	23.23
H15	47.5 U/S	152.50	62.50,64.40	21.88	25.78
H16	24.00 U/S	152.44	86.00,64.44	50.33	50.89
H17	4.00 U/S	152.40	106.00,64.21	71.81	77.04
H18	47.5 U/S	144.30	62.50,56.30	114.97	119.24
H19	24.00 U/S	144.50	86.00,56.30	132.63	138.05
H20	4.00 U/S	144.52	106.00,56.52	128.22	130.12

Table 11: Comparison between the direct measurement of pressure head and SEEP/W for CH 1000

Piezometer number	Offset from the center line (m)	Elevation	Coordinates on the SEEP/W solution	Manually Measured Pressure Head (m)	SEEP/W Computed Pressure Head (m)
H21	3.4U/S	166.98	107.66,77.96	-28.93	-25.14
H22	0.0	167.03	110.00,77.87	-37.88	-34.69
H23	5.0 U/S	158.99	105.00,70.00	31.68	33.96
H24	0.00 U/S	158.99	110.00,70.00	7.68	7.75
H25	6.0 U/S	158.99	117.00,70.00	48.41	51.24
H26	47.5 U/S	152.50	62.50,63.99	76.06	81.85
H27	24.0 U/S	152.44	86.00,64.08	87.97	90.33
H28	4.0 U/S	152.40	106.00,64.21	82.75	83.70
H29	47.5 U/S	144.30	62.50,56.00	164.52	167.60

Table 15 to 17 revealed the results of the pressure head at points on which hydraulic piezometers are installed. The results are compared to those of the manually measured ones. The comparison was made to hydraulic piezometers readings recorded in July, 2007. The comparison revealed a wide margin between the software results and the measured results in some cases and a little margin in other. However, the pattern of increase and decrease from one hydraulic piezometer to another is almost the same.

3.5 Piping

Piping through an embankment dam is said to occur if the hydraulic gradient is equal to or greater than unity. It is expected to occur through the highly permeable embankment material. The highly permeable material is that of the shell and the upper layer of foundation for their hydraulic conductivities being $1.00E-06$ m/s. Nodes information are collected from the six sections studied. Reservoir elevation of 170.97m is considered for being the highest which also produced highest magnitudes of both hydraulic velocities and seepage fluxes. Consideration is made on portions of the sections that have higher concentrations of velocity vectors. The hydraulic gradients are tabulated below.

Table 12: Top 20 Nodal Hydraulic Gradients

CH 600		CH 685		CH 800		CH 880		CH 1000		CH 1100	
Node	Gradient	Node	Gradient	Node	Gradient	Node	Gradient	Node	Gradient	Node	Gradient
988	0.5336	988	0.5336	979	0.4561	979	0.4561	994	0.4324	987	0.3745
1005	0.4715	1005	0.4715	995	0.4861	995	0.4861	1011	0.4324	1003	0.3747
1007	0.5498	1007	0.5498	1011	0.6761	1011	0.6761	1012	0.3847	1020	0.5287
1020	0.5104	1020	0.5104	1013	0.5670	1013	0.5670	1025	0.2631	1024	0.4220
1022	0.7491	1022	0.7491	1029	0.7560	1029	0.7560	1027	0.6120	1040	0.5729
1039	0.8149	1039	0.8149	1045	0.5605	1045	0.5605	1029	0.4863	1042	0.5978
1055	0.9466	1055	0.9466	1046	0.8430	1046	0.8430	1046	0.6651	1055	0.4213
1056	0.6252	1056	0.6252	1062	0.6555	1062	0.6555	1062	0.4876	1058	0.6215

1072	0.7337	1072	0.7337	1075	0.4835	1075	0.4835	1063	0.7230	1074	0.4851
1088	0.8550	1088	0.8550	1079	0.7471	1079	0.7471	1080	0.5630	1075	0.6698
1089	0.5482	1089	0.5482	1093	0.5937	1093	0.5937	1094	0.4087	1089	0.5620
1104	0.6780	1104	0.6780	1107	0.8188	1107	0.8188	1096	0.6535	1093	0.7952
1121	0.8062	1121	0.8062	1109	0.4577	1109	0.4577	1113	0.5134	1106	0.4419
1122	0.5226	1122	0.5226	1111	0.6957	1111	0.6957	1129	0.3871	1108	0.6666
1137	0.6595	1137	0.6595	1127	0.5730	1127	0.5730	1130	0.6248	1124	0.5368
1156	0.5445	1156	0.5445	1129	0.7883	1129	0.7883	1145	0.5013	1129	0.4306
1157	0.7792	1157	0.7792	1144	0.4783	1144	0.4783	1163	0.6028	1141	0.6424
1172	0.6689	1172	0.6689	1145	0.6697	1145	0.6697	1164	0.4127	1147	0.5172
1188	0.3711	1188	0.3711	1161	0.5819	1161	0.5819	1180	0.5123	1164	0.4391
1190	0.6036	1190	0.6036	1177	0.5339	1177	0.5339	1198	0.4716	1182	0.4031

IV.CONCLUSIONS

The seepage analysis conducted on Kiri dam using a software, SEEP/W indicated that the dam is safe in terms of seepage. Seepage fluxes in the sections studied have their magnitudes all in fraction of 6 decimal places. As a result, the annual seepage computed for 1984, 1997 and 2003 are 17,152,165m³, 17,463,865m³ and 17,270,120m³ respectively. These figures are respectively representing 2.779%, 2.840% and 2.808% loss of water in 1984, 1997 and 2003 from the reservoir that meant to impound 615 million cubic meters. The velocity vectors are computed by the software and were found to be by-passing clay core and the diaphragm wall for the less permeability. The pore-water pressure is computed to be uniformly distributed started from the right end of the crest to the bottom left side of the foundation. The computed pore-water pressures have the same growing pattern with the measured one but differ on magnitudes. Piping is not occurring for the fact that phreatic line is not cutting the downstream face and hydraulic gradients are all less than one.

REFERENCES

- [1]. Arora, K. R. (2001). Irrigation, water Power and Water Resources Engineering: Naisarak India: Standard Publishers.
- [2]. ASCE Task Committee. (2000). Artificial Neural Networks in Hydrology, II: Hydrologic Applications 5(2).
- [3]. Aubertin, M., Mbonimpa, M., Bussiere, B., and Chapuis, R.P. (2003). A Model to Predict the Water Retention Curve from Basic Geotechnical Properties. Canadian Geotechnical Journal, 40(6)
- [4]. Beheshthi, A., Kamanbedast, A., and Akbari, H.(2013). Seepage Analysis of Rock Fill Dam Subjected to Water Level fluctuation: A Case Study of Gotvand-Oly Dam.Iranica Journal of Energy and Environment 4(2): 155-160, 2013.
- [5]. Bennett, P.T. (1946). The Effect of Blanket on Pervious Foundation. Trans. ASCE 3: 52-61
- [6]. Billstein, M., Sevansson, U., and Johansson, N.(1999). "Development and Validation of a Numerical Model of Flow through Embankment Dams - Comparisons with Experimental Data and Analytical Solutions", Transport in Porous Media, Vol. 35, No. 3,
- [7]. Boer, S.A and Molen, W.H. (1972). Electrical Models: Conductive Sheet Analogies. Drainage Principles and Application, International Institute for land Reclamation and Improvement. Wageningen, Netherlands Publication 16(1).
- [8]. Bowles, J. E. (1970). Engineering Properties of Soils and Their Measurement. New York: Mcgraw-Hills.
- [9]. Brand, E.W. and Armstrong R. (1968). Sand Model Studies of Seepage through Earth Dams. Proceedings, Symposium on Earth and Rockfill Dams. Indiana. Vol. 1. (pp. 188-196). Indian Press.
- [10]. Casagrande, A. (1937). Seepage through dams, Journal of New England water works, 51,295-336
- [11]. Cedergren, H.R. (1977). Seepage, Drainage and Flow Nets, Wiley. ISBN 0-471-14179-8
- [12]. Craig, R. F (2004). Craig's soil Mechanics. (7th Edition). London and New York Spon Press.
- [13]. Darbandi, A., Torabi, S. O., Saadat, M., Daghighi, Y., and Jarrahbashi, D. (2007). A Moving- Mesh Finite-Volume Method to Solve Free-Surface Seepage Problem in Arbitrary Geometries. International journal for Numerical and Analytical Methods in Geomechanics.
- [14]. Desai, C.S. and Kuppusamy, T. (1980). Development of Phreatic Surface in Earth Embankments. Report Prepared for the Bureau of Reclamation, Department of Civil Engineering, Virginia Polytechnic Institute, Blacksburg, Va.
- [15]. Fakhari, A. and Ghanbari, A. (2013). A Simple Method of Calculating Seepage from Earth Dams. Journal of GeoEngineering 8(1), 27-32. 2013.
- [16]. Fredlund, D.G., Xing, A. and Huang, S. (1994). Predicting the permeability function for Unsaturated Soils using the Soil-water Characteristics curve. Canadian Geotechnical Journal 31(3)
- [17]. GEO-SLOPE (SEEP/W, 2007) Operation Guide for Finite Element Seepage Analysis

- [18]. Geosense Ltd (2014). Application Guide – Piezometers, Version 1.0
- [19]. GGU (Grønlands Geologiske Undersøgelse, 2012). GGU Software.com
- [20]. Goharnejad, H., Noury, M., Noorzad, A., Shamsair, A., and Goharnejad, A. (2016). The Effect of Clay Blanket Thickness to Prevent Seepage in Dam Reservoir.
- [21]. Harr, M.E. (1962) Groundwater and Seepage (2nd Ed.) Mc Graaw-Hill, New York
- [22]. Horace, L. (1993). Hydrodynamics. Cambridge University Press.
- [23]. Hubbert, M. K. (1940). The theory of ground water motion. The journal of Geology 48.
- [24]. Lee, J (2015). Analysis of Measured Seepage Rate of Rock Fill Dams Affected by Changes in Rain Fall for Dam Safety in Korea.
- [25]. Long, P,Jingliang, W. and Qiding, Z. (1995) methods with high accuracy for finite probability computing. Journal of computation and applied mathematics.
- [26]. McAnear, C.L. and Trahan C.C. (1972). Three Dimensional Seepage Model Study, Oakley Dam, Illinois. Miscellaneous Paper S-72-3
- [27]. Mizuno, M. and Hirose, T. (2008). Instrumentation and monitoring of Dams and reservoirs
- [28]. Muazu, A. H (2001). Performance Assessment of Kiri and Dadin Kowa Dams. Unpublished PGD Thesis, Abubakar Tafawa BAlewa University, Bauchi, Nigeria
- [29]. National Dam Safety Program Research Needs Workshop (2006).
- [30]. Omofunmi O. E., Kolo J. G., Oladipo A. S., Diabana P. D., and Ojo A. S.(2017). A Review on Effects and Control of Seepage through Earth-fill Dam. Current Journal of Applied Science and Technology. Pp 2
- [31]. Oosterbaan, R.J. and Nijland H. J. (1994). Drainage Principles and Applications, International Institute for Land Reclamation and Improvement, Publication 16, ISBN 90 70754 33
- [32]. Oosterbaan, K. R. and Nijland H. J. (1994). Determining the Saturated Hydraulic Conductivity. International institute of Land Reclamation and Improvement. Publication 16, Wageningen, the Netherlands.
- [33]. Punmia, B. C and Lal P. B. B (1992). Irrigation and Water Power Engineering. (12th Ed). Udpur India. Laxmi Telford,
- [34]. Raghunath, H. M. (2006). Hydrology Principle, Analysis and Design: New Age International Ltd Publishers,New Delhi. ISBN (10),81-244-2332-9
- [35]. Rezk, M and Nasr, R (1990). An Experimental Study for Seepage Through an Earth Dam with Cut-off wall Based on an Inclined Base. Alex. Eng. J., Alex. Univ., 29(4) 209-214.
- [36]. Rushton, K.R. and Redshaw, S.C. (1979). Seepage And Groundwater Flow. (1st ed.) Wiley: New York. (208-301)
- [37]. Sazzad, M., Roy, M and Rahman, S. (2015). FEM Based Seepage Analysis through Earth Dams. International Journal of Advanced Structures and Geotechnical Engineering. ISSN 2319-2347, Vol 04, No 3
- [38]. Schaffernak K. (1917). A Simple Method of Calculating Seepage from Earth Dams. Journal of Engineering Vol. 8, No 1.
- [39]. Soleymani, A. and Akhtarapur, A. (2011). Seepage Analysis for Shurijeh Reservoir Dam Using Finite Element Method.
- [40]. Thusyanthan, N. I. and Madabushi S. P. G. (2003). Scaling of Seepage Flow Velocity in Centrifuge Models CUED/D-SOILS/TR326
- [41]. Tukur, A. L., and Mubi, A. M. (2002). Impact of Kiri Dam on the Lower Reaches of River Gongola, Nigeria. GeoJournal, Volume 56, Number 2
- [42]. Udo, R. K.(1970). Geographical Regions of Nigeria. London and University of California Press.
- [43]. Uloko J. O. (2016). Seepage Analysis of Dadin Kowa Dam Using Finite Elements Method. Unpublished M.Eng thesis, Abubakar Tafawa BAlewa University, Bauchi, Nigeria
- [44]. Upper Benue River Basins Development Authority, Yola Development Maps
- [45]. USGS (2007). Scientific Investigation Report 2007-5216
- [46]. WardAshcroft and Parkman Nig. (1977). Design and Construction Report of Kiri Dam.

Ahmed Bafeto Mohammed "Seepage Analysis of Kiri Dam Using Finite Elements Method" The International Journal of Engineering and Science (IJES), 8.11 (2019): 66-86